Roles of the Proximal Heme Thiolate Ligand in Cytochrome $P450_{cam}$

Karine Auclair,[†] Pierre Moënne-Loccoz,[‡] and Paul R. Ortiz de Montellano*[,†]

Contribution from the Department of Pharmaceutical Chemistry, University of California, San Francisco, California 94143-0446, and Department of Biochemistry and Molecular Biology, Oregon Graduate Institute of Science and Technology, Beaverton, Oregon 97006-8921

Received November 20, 2000

Abstract: To examine the roles of the proximal thiolate iron ligand, the C357H mutant of $P450_{cam}$ (CYP101) was characterized by resonance Raman, UV, circular dichroism, and activity measurements. The C357H mutant must be reconstituted with hemin for activity to be observed. The reconstituted enzyme is a mixture of high and low spin species. Low temperature (10 °C), low enzyme concentration (1 μM**)**, high camphor concentration (1 mM), and 5−50 mM buffer concentrations increase the high to low spin ratio, but under no conditions examined was the protein more than 60% high spin. The C357H mutant has a poorer K_m for camphor (23 vs 2 μM) and a poorer K_d for putidaredoxin (50 vs 20 μM) than wild-type $P450_{cam}$. The mutant also exhibits a greatly decreased camphor oxidation rate, elevated uncoupling rate, and much greater peroxidase activity. Electron transfer from putidaredoxin to the mutant is much slower than to the wild-type even though redox potential measurements show that the electron transfer remains thermodynamically favored. These experiments confirm that the thiolate ligand facilitates the O−O bond cleavage by P450 enzymes and also demonstrate that this ligand satisfies important roles in protein folding, substrate binding, and electron transfer.

Introduction

Cytochrome P450 (P450) enzymes constitute a family of heme-containing monooxygenases named for their Soret absorption maximum at 450 nm when reduced in the presence of CO. They undergo a denaturing transition to a stable but inactive species known as cytochrome P420 because the absorption maximum of the resulting Fe^{II}-CO complex is at 420 nm. These ubiquitous enzymes are involved in a diversity of vital processes, including drug metabolism, carcinogenesis, degradation of xenobiotics, and the biosynthesis of steroids, lipids, and secondary metabolites. They do so by catalyzing a range of oxidative transformations such as carbon hydroxylation, heteroatom oxidation, and double bond epoxidation. High resolution structures have been reported for several P450 enzymes, including $P450_{cam}$,[2] $P450_{BM-3}$,[3,4] $P450_{terp}$,[5] $P450_{eryF}$,[6,7] $P450_{nor}$,[8] CYP119,[9] and CYP2C5.[10] In the case of $P450_{cam}$, structures have been determined for the substrate-free and camphor-bound enzyme,[2,11] the CO−substrate−enzyme ternary complex,[12] and several additional substrate complexes and point mutants.[13−15] The $P450_{cam}$ catalytic cycle consists of (a) substrate binding with a concomitant increase in the reduction potential of the heme iron atom, (b) reduction of the iron from the ferric to the ferrous state, (c) formation of the ferrous dioxy ($Fe^{II}-O_2$) complex, (d) reduction of the $Fe^{II}-O_2$ complex to a ferric peroxo ($Fe^{III}-OOH$) species, (e) cleavage of the $Fe^{III}-OOH$ dioxygen bond to give a ferryl (formally $Fe^{V}=O$) species, (f) insertion of the ferryl oxygen into a carbon−hydrogen bond of the substrate, and (g) dissociation of the product (Figure 1). Crystal structures have recently been determined for several $P450_{cam}$ intermediates along this pathway.[16,17]

Electron transfer is often rate limiting in P450 catalysis,[18] but the electron transfer process remains poorly understood. Electron transfer from NADH (or NADPH) to P450 is mediated by proteins that can act as single electron donors. In the case of $P450_{cam}$, the physiological partners are the flavoprotein putidaredoxin reductase (PdR) and the iron−sulfur protein putidaredoxin (Pd).[19] Before electron transfer can occur, Pd must bind to $P450_{cam}$ via electrostatic and hydrophobic interactions[20] and some rearrangement or conformational change, as suggested by the observation of a lag phase,[18] must take place. This process

* To whom correspondence should be addressed at the University of California. Fax: 415-502-4728. E-mail: ortiz@cgl.ucsf.edu.
† University of California.
‡ Oregon Graduate Institute of Science and Technology.

(1) Ortiz de Montellano, P. R. In *Cytochrome P450: Structure, Mechanism, and Biochemistry*, 2nd ed.; Plenum: New York, 1995.
(2) Poulos, T. L.; Finzel, B. C.; Howard, A. J. *J. Mol. Biol.* **1987**, *192*, 687−700.
(3) Ravichandran, K. G.; Boddupalli, S. S.; Hasemann, C. A.; Peterson, J. A.; Deisenhofer, J. *Science* **1993**, *261*, 731−736.
(4) Li, H.; Poulos, T. L. *Acta Crystallogr.* **1994**, *D51*, 21−32.
(5) Hasemann, C. A.; Ravichandran, K. G.; Peterson, J. A.; Deisenhofer, J. *J. Mol. Biol.* **1994**, *236*, 1169−1185.
(6) Cupp-Vickery, J.; Li, H.; Poulos, T. L. *Proteins* **1994**, *20*, 187−201.
(7) Cupp-Vickery, J.; Poulos, T. L. *Nat. Struct. Biol.* **1995**, *2*, 144−153.
(8) Shimizu, H.; Park, S.-Y.; Gomi, Y.; Arakawa, H.; Nakamura, H.; Adachi, S.-I.; Obayashi, E.; Iizuka, T.; Shoun, H.; Shiro, Y. *J. Biol. Chem.* **2000**, *275*, 4816−4826.
(9) Yano, J. K.; Koo, L. S.; Schuller, D. J.; Li, H.; Ortiz de Montellano, P. R.; Poulos, T. L. *J. Biol. Chem.* **2000**, *275*, 31086−31092.
(10) Williams, P. A.; Cosme, J.; Sridhar, V.; Johnson, E. F.; McRee, D. E. *Mol. Cell* **2000**, *5*, 121−131.
(11) Poulos, T. L.; Finzel, B. C.; Howard, A. J. *Biochemistry* **1986**, *25*, 5314−5322.
(12) Raag, R.; Poulos, T. L. *Biochemistry* **1989**, *28*, 7586−7592.
(13) Raag, R.; Poulos, T. L. *Biochemistry* **1989**, *28*, 917−922.
(14) Raag, R.; Poulos, T. L. *Biochemistry* **1991**, *30*, 2674−2684.
(15) Raag, R.; Martinis, S. A.; Sligar, S. G.; Poulos, T. L. *Biochemistry* **1991**, *30*, 11420−11429.
(16) Poulos, T. L.; Raag, R. *FASEB* **1992**, *6*, 674−679.
(17) Schlichting, I.; Berendzen, J.; Chu, K.; Stock, A. M.; Maves, S. A.; Benson, D. E.; Sweet, R. M.; Ringe, D.; Petsko, G. A.; Sligar, S. G. *Science* **2000**, *287*, 1615−1622.
(18) Hintz, M. J.; Peterson, J. A. *J. Biol. Chem.* **1981**, *256*, 6721−6728.
(19) Katagiri, M.; Ganguli, B. N.; Gunsalus, I. C. *J. Biol. Chem.* **1968**, *243*, 3543−3546.
(20) Geren, L.; Tuls, J.; O'Brien, P.; Millett, F.; Peterson, J. A. *J. Biol. Chem.* **1986**, *261*, 15491−15495.

10.1021/ja0040262 CCC: $20.00
Published on Web 05/02/2001

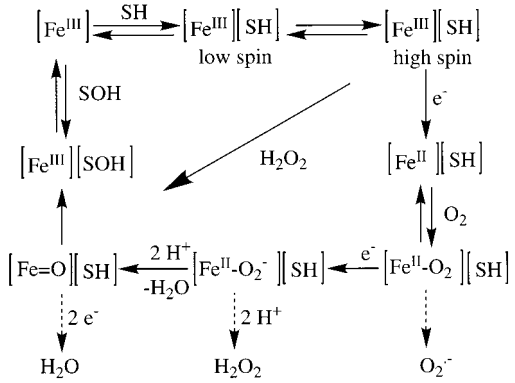

Figure 1. The P450 substrate hydroxylation cycle (full arrows) and the uncoupling pathways (dashed arrows).

results in the transfer of a single electron and presumably must be repeated for the second electron transfer.

The unique monooxygenase activity of P450 enzymes has been largely attributed to the presence of a proximal thiolate heme ligand provided by a deprotonated cysteine residue.[21,22] This unusual ligand is found only in a few other enzymes, most notably chloroperoxidase[23,24] and the nitric oxide synthases.[25,26] The majority of heme-containing enzymes, including all other known peroxidases, have a proximal histidine iron ligand. P450 enzymes are active only when the proximal cysteine ligand is deprotonated, whereas both neutral histidine[27,28] and histidinate[29,30] ligands have been observed in catalytically active hemoproteins. The proximal thiolate ligand of chloroperoxidase, Cys-29, has reportedly been replaced with a histidine residue and the recombinant protein found to retain most of its chlorination, peroxidation, epoxidation, and catalase activities.[31] Conversely, the proximal histidine ligand of several hemoproteins has been replaced by a cysteine, in most cases with a loss or severe reduction of catalytic activity. Thus, for heme oxygenase[32] and cytochrome *c* peroxidase,[33] replacement of the histidine heme iron ligand by a cysteine yields inactive enzymes. However, when the same mutation is introduced into myoglobin, a normally noncatalytic hemoprotein, its low H_2O_2-dependent styrene epoxidase, *N*-demethylase, and catalase activities are reportedly retained.[34,35]

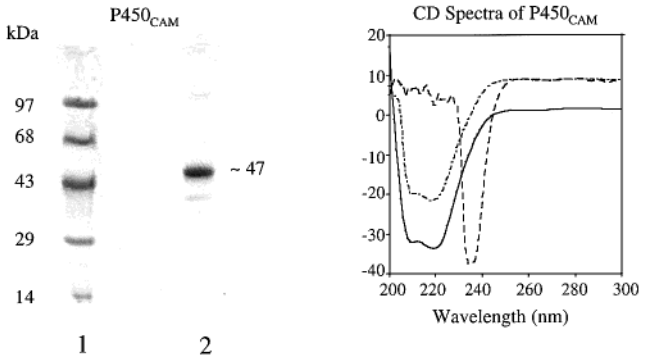

Figure 2. (A) SDS-PAGE on a 12.5% homogeneous Phastgel of the purified C357H $P450_{cam}$ protein. From left to right: lane 1, high molecular weight ladder; lane 2, C357H protein after purification (~47 kDa). (B) Circular dichroism spectra. The wild-type $P450_{cam}$ (—) has minima at 211 and 220 nm. The C357H mutant before reconstitution (- - -) has a single minimum at 235 nm. After reconstitution, the C357H variant (· - · - ·) shows bands at the same wavelengths (210 and 218 nm) as the wild-type. In each case, 1 μM of enzyme was used with 100 μM of camphor in 10 mM potassium phosphate buffer at room temperature.

$P450_{cam}$ was chosen to explore the role(s) of the proximal cysteine ligand because it has served as the prototype for most of the mechanistic and structural advances made in the field. We report here the preparation, characterization, and catalytic activity of the proximal C357H mutant of $P450_{cam}$. Interestingly, after hemin reconstitution/folding, the $P450_{cam}$ C357H mutant hydroxylates camphor, albeit at a much lower rate than the wild-type enzyme. The rate of uncoupling and the K_m for the substrate are greatly increased by the C357H mutation, whereas the rate of electron transfer is dramatically decreased. The results indicate that the cysteine iron ligand has multiple roles in P450 enzymes.

Results

Purification and Reconstitution of the $P450_{cam}$ C357H Mutant. Due to slight differences in chromatographic properties and extended proteolysis, the procedure reported for the purification of $P450_{cam}$ had to be modified to purify the C357H mutant. After purification (Figure 2), the C357H mutant was not as red as wild-type $P450_{cam}$ and did not exhibit the band at 420 nm for the reduced-CO enzyme complex expected of a histidine-ligated hemoprotein. Quantitation of total protein content with the Bio-Rad DC protein assay (based on the Lowry procedure) and of heme-bound protein using as an approximation the extinction coefficient reported for $P450_{cam}$ revealed that the C357H protein preparation contained roughly 1% heme-bound enzyme. In accordance with this low heme content, the consumption of NADH in the presence of Pd, PdR, and camphor was very close to the background level. Clearly, the purified C357H variant was present primarily as the apoenzyme. The protein was therefore reconstituted with hemin.

In earlier studies, apo$P450_{cam}$ has been prepared by removal of the heme in various ways, including acid/acetone precipitation and acid/butanone extraction.[36,37] Hemin reconstitution has only been successfully achieved with $P450_{cam}$.[38] For the C357H mutant discussed here, the hemin reconstitution procedure

(21) Poulos, T. L.; Finzel, B. C.; Gunsalus, I. C.; Wagner, G. C.; Kraut, J. *J. Biol. Chem.* **1985**, *260*, 16122−16128.
(22) Dawson, J. H. *Science* **1988**, *240*, 433−439.
(23) Dawson, J. H.; Sono, M. *Chem. Rev.* **1987**, *87*, 1257−1273.
(24) Sundaramoorthy, M.; Terner, J.; Poulos, T. L. *Structure* **1995**, *3*, 1367−1377.
(25) Crane, B. R.; Arvai, A. S.; Ghosh, D. K.; Wu, C.; Getzoff, E. D.; Stuehr, D. J.; Tainer, J. A. *Science* **1998**, *279*, 2121−2126.
(26) Raman, C. S.; Li, H.; Martásek, P.; Král, V.; Masters, B. S. S.; Poulos, T. L. *Cell* **1998**, *95*, 939−950.
(27) Franzen, S.; Roach, M. P.; Chen, Y.-P.; Dyer, B.; Woodruff, W. H.; Dawson, J. H. *J. Am. Chem. Soc.* **1998**, *120*, 4658−4661.
(28) Seibold, S. A.; Cerda, J. F.; Mulichak, A. M.; Song, I.; Garavito, M.; Arakawa, T.; Smith, W. L.; Babcock, G. T. *Biochemistry* **2000**, *39*, 6616−6624.
(29) Finzel, B. C.; Poulos, T. L.; Kraut, J. *J. Biol. Chem.* **1984**, *250*, 13027−13036.
(30) Smulevich, G.; Hu, S.; Rodgers, K. R.; Goodin, D. B.; Smith, K. M.; Spiro, T. G. *Biospectroscopy* **1996**, *2*, 365−376.
(31) Yi, X.; Mroczko, M.; Manij, K. M.; Wang, X.; Hager, L. P. *Proc. Natl. Acad. Sci. U.S.A.* **1999**, *96*, 12412−12417.
(32) Liu, Y.; Moënne-Loccoz, P.; Hildebrand, D. P.; Wilks, A.; Loehr, T. M.; Mauk, A. G.; Ortiz de Montellano, P. R. *Biochemistry* **1999**, *38*, 3733−3743.
(33) Choudhury, K.; Sundaramoorthy, M.; Mauro, J. M.; Poulos, T. L. *J. Biol. Chem.* **1994**, *267*, 25656−25659.
(34) Adachi, S.; Nagano, S.; Ishimori, K.; Watanabe, Y.; Morishima, I.; Egawa, T.; Kitagawa, T.; Makino, R. *Biochemistry* **1993**, *32*, 241−252.
(35) Hildebrand, D. P.; Ferrer, J. C.; Tang, H.-L.; Smith, M.; Mauk, A. G. *Biochemistry* **1995**, *34*, 11598−11605.
(36) Yu, C.-A.; Gunsalus, I. C. *J. Biol. Chem.* **1974**, *249*, 107−110.
(37) Wagner, G. C.; Perez, M.; Toscano, W. A., Jr.; Gunsalus, I. C. *J. Biol. Chem.* **1981**, *256*, 6262−6265.
(38) Attempts to carry out analogous studies of the corresponding $P450_{BM-3}$ thiolate to histidine (C400H) mutant were unsuccessful because the apoprotein obtained from the expression system could not be reconstituted into the heme-bound form.

Table 1. Optimization of the High Spin/Low Spin Ratio of C357H

parameters	optimum high/low spin P450$_{cam}$	optimum high/low spin C357H
time	unchanged for >30 min	unchanged for >30 min
temperature	30−45 °C	5−15 °C
pH	7.4 broad	7.4 sharp
buffers: KPi, Tris, Mops, HEPES, NH_4Ac, or citrate	unchanged	unchanged
camphor concentration	plateau ≥60 μM	plateau >200 μM (erratic)
imidazole concentration	100 μM displaces 80% of camphor (100 μM)	100 μM displaces 80% of camphor (100 μM)
buffer (KPi) concentration	>100 mM	5−50 mM
enzyme concentration	>10 μM	<10 μM

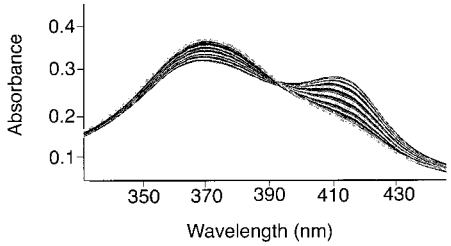

Figure 3. Titration of the C357H P450$_{cam}$ mutant with camphor (0 to 500 μM) in 10 mM potassium phosphate buffer at pH 7.4 and room temperature. As camphor is added the absorption at 418 nm increases, while that at 368 nm decreases. This experiment strongly suggests that the high spin and low spin species have absorption maxima of 418 and 368 nm, respectively.

reported for apoP450$_{cam}$ and a procedure utilized for the reconstitution of heme oxygenase[39] were run in parallel and the extent of reconstitution followed for a period of up to one week. Heme oxygenase, which has a histidine iron ligand, has to be reconstituted with heme after purification since it physiologically degrades heme to biliverdin, iron, and CO.[39] The heme oxygenase procedure, with the addition of camphor, was definitely found to be superior and resulted in maximum reconstitution within 18 h. Circular dichroism spectroscopy (Figure 2) reveals that the reconstitution involves not only binding of hemin but also folding of the protein.

Low Spin/High Spin Equilibrium of the C357H Mutant. Interestingly, after hemin reconstitution of C357H P450$_{cam}$, removal of excess hemin using a hydroxyapatite column yielded two red bands: band 1 coming out during the wash with 5 mM potassium phosphate buffer and band 2 at approximately 100 mM buffer. The two bands display very similar properties. When band 1 is loaded back onto a fresh hydroxyapatite column, two red bands, bands 1.1 and 1.2, again result and the same phenomenon is observed when band 1.1 is loaded onto a fresh hydroxyapatite column on that same day. Loading band 2 onto a fresh hydroxyapatite column after dialysis also leads to two red bands, bands 2.1 and 2.2, the second of which behaves the same way when run, again after dialysis, through a fresh column. After each column, the protein identity and purity were verified by SDS-PAGE and were found to be constant and identical. A possible explanation for this phenomenon is a slow equilibrium between the high and low spin forms of the protein. A fast equilibrium would not produce two sharp bands but rather one or two long streaking band(s). This equilibrium hypothesis was tested by careful UV−vis analysis of the column fractions. As elution progresses for band 1, a slow increase in absorbance at 368 nm parallels a decrease at 418 nm, and the same is observed for band 2. On the basis of binding studies (Figure 3), the absorption at 368 nm is believe to be due to the low spin state of C357H, whereas the high spin state absorbs at 418 nm. These absorption maxima differ from those for the wild-type enzyme, for which the low and high spin species have maxima at 416 and 392 nm, respectively. The chromatographic separation of the low and high spin species is further confirmed when a roughly 1:1 mixture of high and low spin wild-type P450$_{cam}$ obtained with a limited amount of camphor is eluted through a fresh hydroxyapatite column. As found for the C357H mutant, two red bands elute separately, corresponding to a mostly high spin form (band 1) and a predominantly low spin form (band 2), as determined by UV−vis spectroscopy. From these experiments it is concluded that the two bands observed on the hydroxyapatite column after reconstitution of the C357H mutant represent a mixture of high and low spin species in slow equilibrium.

An elevated high spin/low spin ratio of the C357H mutant is desired as it is expected to enhance the enzyme activity. The effects of time, temperature, pH, and buffer on this ratio are displayed in Table 1. The concentrations of camphor, imidazole, enzyme, and buffer all affect the relative amounts of high and low spin species. The optimum concentration of camphor required with the C357H mutant is much higher than that for wild-type P450$_{cam}$, and much lower temperatures are required to attain the maximum C357H high spin/low spin ratio, which suggests that the mutant is more flexible. The spin state shift produced by camphor is reversed by the addition of 100 μM imidazole, which fully displaces the substrate from both enzymes. The effect of enzyme concentration indicates potential deleterious protein interactions. Surprisingly, in the absence of camphor, the C357H mutant still consists of a mixture of high and low spin states, whereas the wild-type enzyme is exclusively in the low spin form. Unfortunately, it was not possible to convert the C357H mutant to a predominantly high spin species under any conditions.

Resonance Raman. Resonance Raman (RR) spectroscopy was used to further characterize the C357H mutant. Prior to hemin reconstitution, no heme RR signal could be detected with the mutant protein. However, after heme incorporation the mutant protein displayed high-quality RR spectra with Soret excitation. In the ferric state, the high-frequency RR spectra are indicative of a mixture of five-coordinate high spin (5cHS) and six-coordinate low spin (6cLS) species with ν_3 at 1490 and 1502 cm^{-1} and ν_2 at 1575 and 1583 cm^{-1}, respectively (Figure 4A). The RR spectrum of the ferrous state produced by anaerobic addition of dithionite also presents a HS/LS mixture with ν_3 at 1470 and 1492 cm^{-1}, respectively (Figure 4B). The Fe^{II}−His stretching vibrations usually occur between 200 and 250 cm^{-1} but none were detected in the RR spectrum of the C357H mutant. In part, this may be due to the spin state equilibrium observed with this mutant, since the Fe^{II}−His stretching vibrations are resonance enhanced only for HS species. In addition to this spin state dependence, the resonance enhancement of ν(Fe^{II}−His) is strongly dependent on the

(39) Wilks, A.; Black, S. M.; Miller, W. L.; Ortiz de Montellano, P. R. *Biochemistry* **1995**, *34*, 4421−4427.

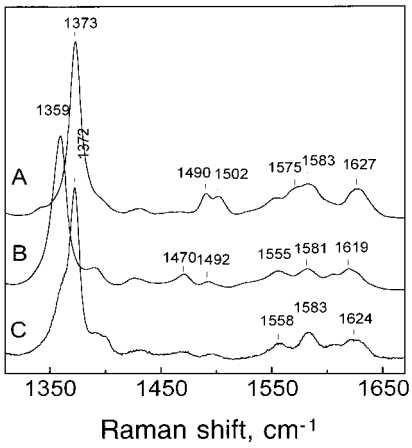

Figure 4. High frequency region of the RR spectra of the ferric (A), ferrous (B), and ferrous−CO complex (C) of the C357H mutant at a 250 μM concentration in 50 mM phosphate buffer, pH 7.4, with 100 μM camphor. Spectra were obtained at room temperature with 413-nm excitation.

excitation wavelength.[40] For example, in deoxymyoglobin the ν(Fe^{II}−His) is best observed with a laser excitation red-shifted from the Soret maximum and is likely to involve an underlying CT band. Such a CT band may be weaker or shifted in the mutant protein.

Exposure to CO converts all of the ferrous heme species to carbonyl complexes as demonstrated by an upshift of the intense ν_4 from 1359 cm^{-1} in the Fe^{II} state to 1372 cm^{-1} in the heme−CO complex (Figure 4C). The ν(Fe−CO) and ν(C−O) were found at 494 and 1968 cm^{-1}, respectively (data not shown). The detection of a single set of RR frequencies shows that the C357H heme−CO complex is a homogeneous population and, incidentally, confirms the success of the heme reconstitution procedure. Moreover, through their sensitivity to the proximal ligand trans effect,[41] the ν(Fe−CO) and ν(C−O) frequencies are consistent with a neutral proximal histidine ligand in the C357H mutant as opposed to a nonspecific ligand such as an aqua/hydroxo molecule. Indeed, in hemoproteins where mutation of the proximal histidine has resulted in aqua/hydroxy−heme iron ligation, the ferrous−CO complex has invariably shown a ν(Fe−CO) above 515 cm^{-1}.[31,42−44] The HS/LS equilibrium in the Fe^{III} and Fe^{II} forms is assigned to the presence of a labile sixth ligand that stronger ligands such as CO and O_2 can readily displace.

Camphor Transformation with Pd/PdR/NADH. A rapid way to evaluate the activity of P450 enzymes is to measure their initial rate of NADH/NADPH consumption at 340 nm, although this measurement does not distinguish uncoupled reduction of O_2 to H_2O_2 or H_2O from actual substrate oxidation. The initial rate of NADH consumption of the C357H variant is 17 times less than that of wild-type P450cam at 37 °C and two times less at 10 °C (Table 2). Under our conditions, P450$_{cam}$ oxidizes camphor to 5-*exo*-hydroxycamphor (90%) and 5-ketocamphor (10%). The production of these metabolites was established by gas chromatography (GC) and GC-MS comparison with standard compounds (Figure 5). At 37 °C, more than 90% of the camphor is oxidized by P450$_{cam}$ in less than 30 min, but no products are detected for the reaction with the C357H mutant. When the reaction is assayed with much higher concentrations (200 μM) of the mutant enzyme under conditions that maximize the high spin state (10 °C, 10 mM potassium phosphate, pH 7.4, 1 mM camphor), approximately 1% of the camphor is transformed into 5-*exo*-hydroxycamphor. No 5-

Table 2. Catalytic Properties of Wild-Type P450$_{cam}$ and Its C375H Mutant

	P450$_{cam}$	C357H
initial rate of NADH consumption at 37 °C (μmol NADH min^{-1} mmol^{-1})	500	30 ± 10
k_{cat} total (s^{-1})	34	0.08 ± 0.04
K_m for camphor (μM)	2	23 ± 4
K_d of camphor/enzyme (μM)	1	1 ± 1
K_d of Pd/enzyme (μM)	20	50 ± 4
H_2O_2 production (s^{-1})	0 (<1%)	0.08 ± 0.04
camphor oxidation (s^{-1})	34 (>99%)	(1 ± 0.5) × 10^{-7}

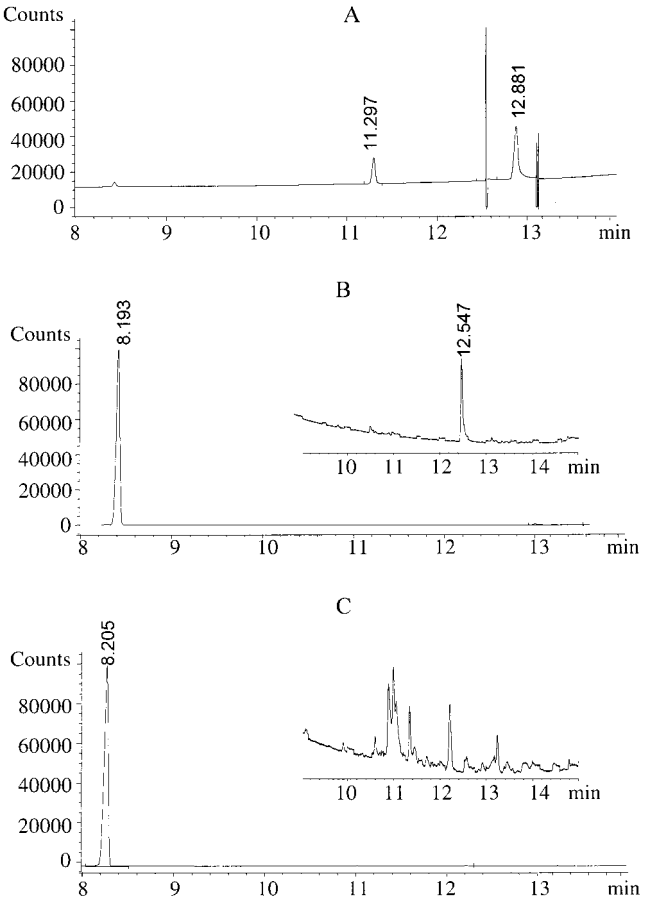

Figure 5. The transformation of camphor as monitored by GC. Under our conditions (Experimental Section), the retention times were 8.4 min for camphor, 11.3 min for 5-ketocamphor, and 12.9 min for 5-*exo*-hydroxycamphor. (A) Chromatogram obtained after the reaction of P450$_{cam}$ (1 μM) with camphor (1 mM) in the presence of Pd (4 μM), PdR (1 μM), and NADH (4 mM) in 50 mM potassium phosphate buffer, pH 7.4, for 30 min at room temperature. More than 95% of the camphor was transformed into products. (B) The reaction of the C357H mutant (~200 μM enzyme was required to detect product formation) performed in the same way but with the addition of catalase (500 μg/mL) to consume H_2O_2 resulting from uncoupling and at 10 °C overnight. (C) Chromatogram obtained after the reaction of the C357H mutant (200 μM) with camphor (1 mM) in the presence of H_2O_2 (700 mM) for 16 h at 10 °C. The insets are magnified approximately 40-fold.

(40) Kitagawa, T. *Heme protein structure and iron-histidine stretching mode*; Spiro, T. G., Ed.; John Wiley & Sons: New York, 1988; Vol. 3, pp 97−131.

(41) Ray, G. B.; Li, X.-Y.; Ibers, J. A.; Sessler, J. L.; Spiro, T. G. *J. Am. Chem. Soc*. **1994**, *116*, 162−176.

(42) Sun, J.; Loehr, T. M.; Wilks, A.; Ortiz de Montellano, P. R. *Biochemistry* **1994**, *33*, 13734−13740.

(43) Wilks, A.; Moenne-Loccoz, P. *J. Biol. Chem*. **2000**, *275*, 11686−11692.

(44) Chu, G. C.; Katakura, K.; Tomita, T.; Zhang, X.; Sun, D.; Sato, M.; Sasahara, M.; Kayama, T.; Ikeda-Saito, M.; Yoshida, T. *J. Biol. Chem*. **2000**, *275*, 175494−17500.

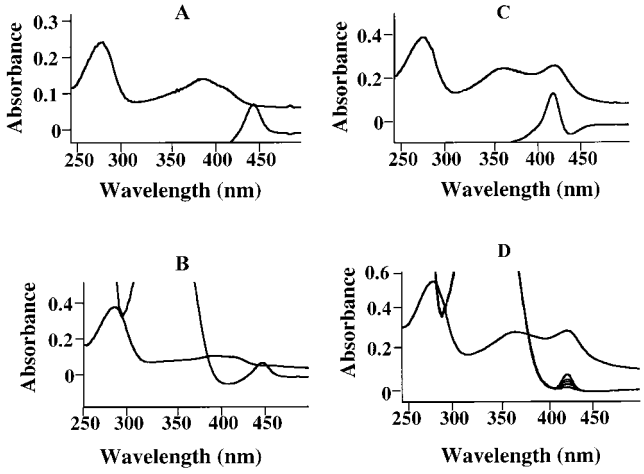

Figure 6. Electron-transfer monitored by UV spectrophotometry. (A) The ferric form of P450$_{cam}$ in the presence of camphor, with maxima at 280 and 392 nm for the 5-coordinate high spin and 416 nm for the 6-coordinate low spin states. The enzyme is reduced from the ferric to the ferrous state with sodium dithionite, and after blanking, CO is bubbled through the solution before the difference spectrum of the Fe^{II}−CO complex is obtained (maximum at ∼450 nm). (B) Spectra of the ferric wild-type enzyme and the Fe^{II}−CO complex obtained by reduction with Pd/PdR/NADH. (C) The Soret bands of the ferric C357H mutant are at 418 and 368 nm for the high and low spin states, respectively. Finally, the Fe^{II}−CO complex of the C357H mutant, obtained by reduction with sodium dithionite, has a maximum absorption at 420 nm. (D) Formation of the Fe^{II}−CO complex of the C357H mutant with Pd/PdR/NADH is much slower than that with sodium dithionite, and much slower than that for the wild-type.

ketocamphor was detected by GC-MS. The K_m values (Table 2), which reflect binding to an activated state of the enzyme, suggest that camphor binds 10-times more poorly to the C357H mutant than to the wild-type enzyme even though the K_d values for the substrate are the same for the ferric wild-type and mutant enzymes. The requirement for reconstitution of the enzyme and the low catalytic activity readily explain why earlier studies did not detect the catalytic activity of the mutant.[45]

Electron Transfer. Figure 6 shows the UV−vis spectra of the ferric, ferrous, and Fe^{II}−CO complexes of the wild-type and the C357H mutant obtained by reduction with either sodium dithionite or NADH/Pd/PdR. The Fe^{II}−CO complexes absorb at 450 when the heme iron ligand is a thiolate and at 420 nm when the ligand is a histidine. Sodium dithionite reduces both the wild-type and the C357H mutant equally well, whereas reduction with NADH/Pd/PdR proceeds much faster with the wild-type than with the C357H mutant. The rate of electron transfer from Pd/PdR/NADH to the C357H mutant was slow enough to be spectroscopically measured and a value of 0.003 s^{-1} was calculated. The reported rate of electron transfer to P450$_{cam}$ measured by stopped-flow spectrophotometry is 30 s^{-1}, that is 10^4 times faster than the mutant.[18,46] This decrease in the rate of electron transfer clearly contributes to the slow turnover of camphor by the mutant enzyme.

Reduction Potential. Electron transfer to the C357H variant was further studied by determining the reduction potentials of the Fe^{III}/Fe^{II} couple of P450$_{cam}$ and its C357H mutant in the presence of camphor and Pd. Figure 7 shows typical spectra obtained during reductive titration in the presence of indigo carmine. The Nernst equation was used to plot the data, and

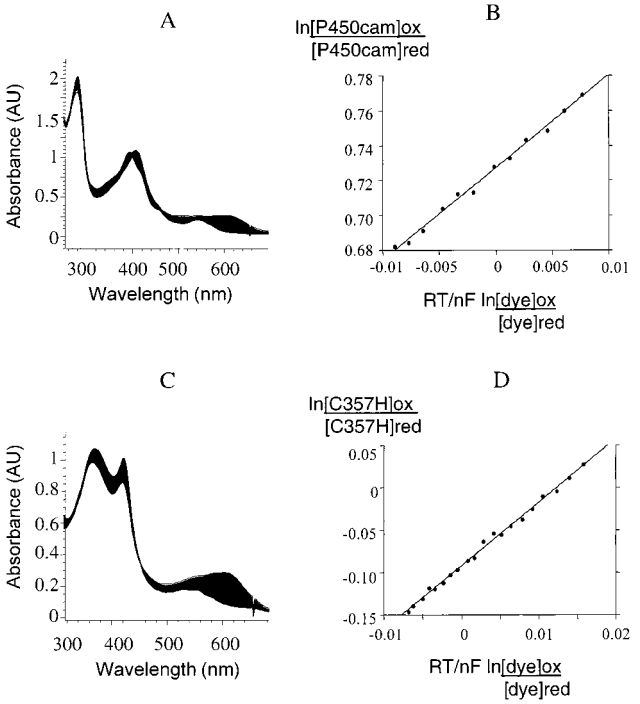

Figure 7. Determination of the reduction potential of wild-type P450$_{cam}$ (A and B) and of its C357H mutant (C and D). Figures B and D only show the linear portions of the titration plots. UV spectra A and C show the decreasing absorption at 608 nm due to the redox dye indigo carmine, as well as the distribution of the Fe^{III} and Fe^{II} forms for the wild-type (392 and 408 nm, respectively) and the mutant (418 and 422 nm, respectively) collected during a typical midpoint potential determination. The Nernst equation was applied to calculate the reduction potential. The concentration of reduced enzyme was determined at one of the putidaredoxin isosbestic points (ϵ_{480} = 25.5 mM^{-1} cm^{-1}) and the midpoint potential was calculated from the *y*-intercept of the log ox/red plot.

from the *y*-intercept, a reduction potential of −177 mV was calculated for P450$_{cam}$, in good agreement with the previously reported value of −173 mV.[47] The measurements obtained for the C357H mutant under the same conditions, using the linear portions of the titration curves, give a reduction potential of −156 mV. Replacement of the cysteine proximal iron ligand of P450$_{cam}$ by a histidine is expected to raise the reduction potential of the iron more than the small increase that is actually observed. As shown in Figure 6, wild-type P450$_{cam}$ was mostly in the high spin state before the titration started. However, it was not possible to similarly shift all of the C357H mutant into the high spin state, so that the reduction potential was measured for an approximately 1:1 mixture of high and low spin species. The reduction potential of the pure high spin mutant species is expected to be significantly higher than the −156 mV calculated, based on the reported redox potentials of low spin wild-type P450$_{cam}$ (−300 mV) and of heme proteins that have a histidine proximal iron ligand.

***K*$_d$ Determination for the Pd/P450$_{cam}$ and Pd/C357H Complexes.** The dissociation constants of Pd with either the wild-type enzyme or its C357H mutant were determined by UV spectroscopy (not shown). The decrease in absorbance at 392 nm for the wild-type and 425 nm for the mutant were followed as Pd was added. The decrease in absorbance was plotted against the ratio of the decrease in absorbance over the concentration of the free ligand. The dissociation constants estimated from

(45) Unger, B. Ph.D. Thesis, University of Illinois at Urbana-Champaign, 1988.

(46) Hintz, M. J.; Mock, D. M.; Peterson, L. L.; Tuttle, K.; Peterson, J. A. *J. Biol. Chem.* **1982**, *257*, 14324−14332.

(47) Sligar, S. G.; Gunsalus, I. C. *Proc. Natl. Acad. Sci. U.S.A.* **1976**, *73*, 1078−1082.

the slopes are 20 μM for the wild-type and 50 μM for the mutant, in agreement with the literature value of 17 μM for the wild type.[48] The affinities of the mutant and the wild-type enzymes for Pd differ modestly and cannot account for the large difference in electron-transfer rates.

Uncoupling Rate. As already mentioned, uncoupling of the reduction of oxygen to produce H_2O_2 and/or H_2O rather than hydroxylated substrate is well established for P450 enzymes.[49−52] The broken arrows in Figure 1 show three routes that lead to uncoupling: (a) decomposition of the $Fe^{II}-O_2$ species to give the ferric enzyme and superoxide, which in turn dismutates to H_2O_2; (b) decomposition of the ferric−peroxide intermediate to directly give the ferric enzyme and H_2O_2; and (c) production of H_2O by reduction of the $[Fe^{V}{=}O]$ species. The production of superoxide, peroxide, and/or water decreases the efficiency of the enzyme by uncoupling NADH consumption from product formation. The hydroxylation of camphor by wild-type $P450_{cam}$ is highly coupled, with more than 99% of the NADH equivalents being used to hydroxylate the substrate. In contrast, a much higher rate of uncoupling is indicated for the C357H mutant by the large difference between the rates of camphor hydroxylation and NADH consumption (Table 2). The iron thiocyanate assay for the determination of H_2O_2 was not sensitive enough to allow accurate determination of this product under our conditions,[53] so the uncoupling of the C357H mutant was investigated by monitoring the horseradish peroxidase-mediated decrease in the fluorescence of scopoletin caused by the formation of H_2O_2.[54] The rate of H_2O_2 production (0.08 s^{-1}, see Table 2) accounts for virtually all of the NADH consumption because the rate of camphor hydroxylation (1×10^{-7} s^{-1}) is a few orders of magnitude smaller than that of H_2O_2 production.

Camphor Transformation with H_2O_2. A shunt pathway exists that bypasses the electron-transfer steps and allows one to assay the oxidative activity of P450 enzymes independent of electron transfer. In the shunt pathway, H_2O_2 reacts with the enzyme to directly form the $Fe^{III}-OOH$ species that is then converted to the ferryl species by protonation and elimination of a molecule of water. The reaction of $P450_{cam}$ (1 μM) with H_2O_2 at room temperature for 30 min converted 20% of the camphor to 5-*exo*-hydroxycamphor and 1% to 5-ketocamphor. Under the same conditions, no camphor products were detected with the C357H mutant. However, when the enzyme concentration was raised to 200 μM and the reaction was run in 10 mM potassium phosphate at 10 °C overnight, 0.5% of the camphor was transformed into the 5-*exo*-hydroxycamphor product (Figure 5). This result clearly shows that a flaw in electron transfer to the iron is not alone responsible for the decreased catalytic activity of the mutant. There is also an impairment in the mechanism of oxygen activation or substrate hydroxylation.

Peroxidase Activity. In P450 enzymes, the proximal iron ligand is a cysteine anion, whereas for most peroxidases the proximal ligand is a histidine. The C357H mutant was found to exhibit a 100-fold higher guaiacol peroxidation activity with H_2O_2 as the cosubstrate than the wild-type enzyme (Figure 8).

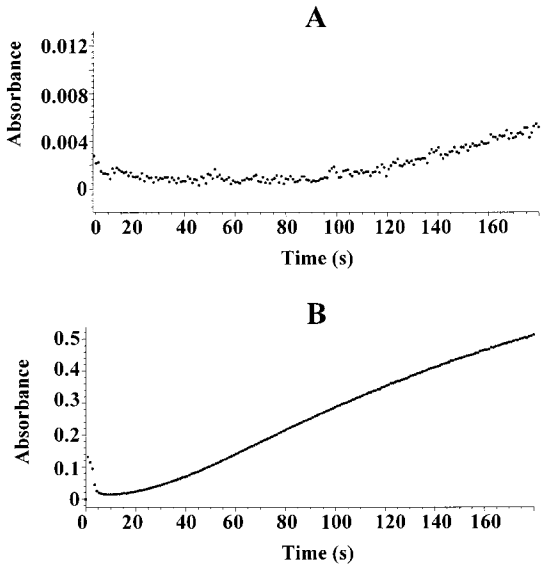

Figure 8. The peroxidase activity of wild-type $P450_{cam}$ (A) and the C357H mutant (B) determined by monitoring the formation of the guaiacol oligomers at 470 nm in the presence of H_2O_2 (2 mM), guaiacol (2 mM), and enzyme (10 μM) in 100 mM potassium phosphate buffer, pH 7.4. The initial slope of the absorbance was used to calculate the peroxidase activity.

Discussion

After purification, heterologously expressed wild-type $P450_{cam}$ is obtained as a properly folded, heme-containing protein. In contrast the C357H mutant is misfolded but can be refolded by appropriate reconstitution with hemin to give a wild-type-like CD spectrum (Figure 2). The UV−vis and RR properties of the protein clearly indicate that the cysteine iron ligand in the C357H mutant has been replaced by a histidine. RR of the CO complex of the $P450_{cam}$ C357H mutant shows that the heme binding site is homogeneous. The high and low spin forms of both the wild-type and the mutant can be partially purified on a hydroxyapatite column, but they slowly equilibrate to a low/high spin mixture, the ratio of which depends on the temperature, the pH, and the camphor, imidazole, enzyme, and buffer concentrations. Unlike the wild-type enzyme, the optimum high/low spin ratio of the mutant is obtained with low concentrations of buffer (low ionic strength) and enzyme, suggesting that charge interactions may be more important for the C357H mutant. The effect of temperature on the C357H mutant is also noteworthy. As the sample is warmed from 10 to 56 °C, there is a gradual partial shift from the high to the low spin state. The highest proportion of the high spin state is obtained at temperatures between 5 and 15 °C. The basis for this temperature dependence is unclear but reflects a destabilization of the high versus low spin states by the mutation, possibly as a consequence of conformational perturbations or increased conformational flexibility of the protein. Although a shift in the spin state is observed for both the wild-type and the mutant as the enzyme is titrated with camphor, a fully high spin state is not reached with the mutant (Figure 3), indicating that the spin states and their dependence on substrate binding are influenced by the nature of the proximal ligand.

Electron transfer from the NADH/PdR/Pd system to the enzyme is 10 000 times slower for the C357H mutant than for the wild-type. This difference in electron-transfer ability is not

(48) Koga, H.; Sagara, Y.; Yaoi, T.; Tsujimura, M.; Nakamura, K.; Sekimizu, K.; Makino, R.; Shimada, H.; Ishimura, Y.; Yura, K.; Go, M.; Ikeguchi, M.; Horiuchi, T. *FEBS Lett.* **1993**, *331*, 109−113.
(49) Sligar, S. G.; Lipscomb, J. D.; Debrunner, P. G.; Gunsalus, I. C. *Biochem. Biophys. Res. Commun.* **1974**, *61*, 290−296.
(50) Zhukov, A. A.; Arachov, A. I. *Biochem. Biophys. Res. Commun.* **1982**, *109*, 813−818.
(51) Kuthan, H.; Ullrich, V. *Eur. J. Biochem.* **1982**, *126*, 583−588.
(52) Gorsky, L. D.; Koop, D. R.; Coon, M. J. *J. Biol. Chem.* **1984**, *259*, 6812−6817.
(53) Wagner, C. D.; Clever, H. L.; Peters, E. D. *Anal. Chem.* **1947**, *19*, 980−982.
(54) Hildebrandt, A. G.; Roots, I.; Tjoe, M.; Heinemeyer, G. *Methods in Enzymology*; Fleischer, S., Packer, L., Eds.; Academic Press Inc.: New York, 1974; Vol 54, pp 342−350.

due to a prohibitive change in the redox potential of the protein, as reduction potentials of −177 (literature −173 mV)[47] and −156 mV were measured in the presence of Pd for the wild-type and C357H enzymes, respectively. The electron transfer thus remains thermodynamically favored in the mutant, as the reduction potential of Pd is −253 mV.[55] It is to be noted that the reduction potentials reported here are for the high spin wild-type enzyme but a 1:1 high:low spin mixture of the mutant. On the basis of the reduction potential of −300 mV for low spin P450$_{cam}$,[47] the reduction potential of the completely high spin C357H variant is expected to be significantly higher than −156 mV. It is difficult to determine whether factors other than the difference in coordination contribute to the difference in reduction potentials because the redox potential depends on various parameters, including the nature of the iron ligands, the spin state, electrostatic interactions of the redox center with charged groups, and the general protein environment.

The observed change in electron-transfer rates could arise from weaker binding of Pd to the C357H P450$_{cam}$ mutant or a change in the ability of Pd to induce the requisite conformational change in the P450 protein.[18] A difference in the binding of Pd might be expected, as the spin state influences the association of P450 enzymes with their redox partners. However, although the K_d value determined here for the Pd/C357H pair is higher than that for Pd/P450$_{cam}$, the difference is relatively small and does not account for the 10 000-fold slower rate of electron transfer. This is true even though the K_d was only determined for the high spin fraction present in the C357H protein mixture (425 nm), whereas the electron-transfer rate was calculated for the mixture of high and low spin forms. Even though the association of the C357H enzyme with Pd is of the same order of magnitude as that of the wild-type, the mutation may still prevent the conformational changes required for electron transfer between P450$_{cam}$ and Pd. Finally, when the Pd concentration exceeds 100 μM during the K_d determination, no further changes are detected for the wild-type protein at 392 nm, but the minimum observed for the mutant slowly shifts from 425 to 418 nm and continues to decrease. This suggests the presence of a second Pd binding site of lower affinity in the C357H mutant that is absent in the wild-type protein.

NADH consumption, as suggested by the slow rate of electron transfer (vide supra), is much lower for the C357H mutant than wild-type P450$_{cam}$ even when the measurements are made under conditions that optimize the C357H high spin form (Table 1). The mutant does, however, oxidize camphor to 5-*exo*-hydroxycamphor in the presence of Pd/PdR/NADH (Figure 5), although nearly all (99.9998%) of the NADH consumed is used to produce H_2O_2 rather than the organic product (Table 2). 5-Ketocamphor, the usual minor product, is not observed with the mutant probably because the production of 5-hydroxycamphor is too low to make it a competitive substrate. Uncoupling is thought to be due to uncontrolled access of solvent molecules to the active site that result in destabilization of the $Fe^{II}-O_2$ and $Fe^{III}-OOH$ complexes. The high ratio of uncoupling versus camphor turnover observed for the mutant thus reflects, in part, slower electron transfer, a perturbed interaction of the enzyme with the substrate indicated by the K_m and spin state changes, and a more stable distal ligand.

The C357H mutation has an additional deleterious impact on the ability of the enzyme to hydroxylate camphor. This is clearly shown by the finding that the activity of the enzyme supported by H_2O_2 rather than NADH/O_2 (Figure 5), an activity independent of exogenous electron transfer, is also impaired by the C357H mutation. This was not unexpected, as electron donation from the thiolate has been proposed to facilitate heterolytic dioxygen bond cleavage.[56−58] The neutral histidine ligand of the C357H mutant presumably does not perform this task as efficiently, although even here small conformational alterations in the active site due to the change in proximal ligand could contribute to the slower rate of reaction with H_2O_2. For this reason, we determined whether the C357H mutant might catalyze alternative reactions. Indeed, the mutant was found to catalyze the peroxidation of guaiacol at a rate 100-times the nearly negligible rate obtained with the wild-type enzyme This acquisition of a new catalytic activity, albeit much lower than that of a true peroxidase, suggests that the ferryl species formed in the C357H mutant is less reactive and thus can carry out side reactions (guaiacol peroxidation) not observed with the wild-type enzyme.

Finally, in this study we mutated the cysteine of P450$_{cam}$ to a histidine to reduce the electron-donating capacity of the proximal iron ligand. During the revision of this manuscript Morishima and co-workers[58] reported a study of a P450$_{cam}$ mutant designed to increase the electron-donating ability of the proximal thiolate ligand. Interestingly, the conclusions reached by the two approaches reinforce each other. We demonstrate here that reduced electronegativity of the proximal ligand decreases coupling at the expense of uncoupling and increases the redox potential of the Fe^{III}/Fe^{II} couple. Morishima and co-workers reported that an increased push effect at the proximal site has the opposite effects.

Conclusions. The results indicate that the proximal cysteine heme iron ligand is not absolutely required for camphor hydroxylation by P450$_{cam}$, although the substrate turnover rate is dramatically reduced and uncoupling accounts for most of the NADH consumed by the mutant. These changes are the result of multiple adjustments associated with the mutation, including a lower K_m for the substrate, an impairment in the substrate-dependent spin state shift, a lower affinity for the Pd redox partner, a greatly decreased rate of electron transfer, a lower stability of the $Fe^{II}-O_2$ and $Fe^{III}-OOH$ intermediates, a reduced ability to cleave the oxygen−oxygen bond to form the ferryl species, and possibly a susceptibility to alternative reactions such as substrate peroxidation. The proximal cysteine heme iron ligand of P450 enzymes thus cannot be viewed simply in terms of its effect on the dioxygen bond cleavage, as is commonly done, but must also be viewed in terms of its role in protein folding, substrate and redox partner binding, coupling/uncoupling partitioning, and electron transfer. Some of these effects are the result of structural changes caused by differences in the size of the cysteine and histidine side-chains, whereas others are the direct result of the change in the nature of the ligand−iron bond.

Experimental Procedures

Materials. The QuickChange site-directed mutagenesis kit and the nitrilotriacetic acid resin (NTA-Agarose) were from Stratagene (La Jolla, CA). The nickel columns were generated by washing the NTA resin with 5 column volumes of 100 mM nickel sulfate. NADH, NADPH, camphor, EDTA, catalase, hemin, xanthine, xanthine oxidase, benzyl viologen, indigo carmine, scopoletin, leupeptin, chymostatin, pepstatin

(55) Aoki, M.; Ishimori, K.; Morishima, I. *Biochim. Biophys. Acta* **1998**, *1386*, 157−167.

(56) Dawson, J. H.; Trudell, J. R.; Barth, G.; Linder, R. E.; Bunnenberg, E.; Djerassi, C.; Chiang, R.; Hager, L. P. *J. Am. Chem. Soc.* **1976**, *98*, 3709−3710.

(57) Dawson, J. H.; Sono, M. *Chem. Rev.* **1987**, *87*, 1255−176.

(58) Yoshioka, S.; Takahashi, S.; Ishimori, K.; Morishima, I. *J. Inorg. Biochem.* **2000**, *81*, 141−151.

A, PMSF, H_2O_2, guaiacol, dithiothreitol, sodium dithionite, β-mercaptoethanol, and DEAE Sepharose were purchased from Aldrich or Sigma. Yeast extract, tryptone, 2YT, imidazole, EDTA, and organic solvents were obtained from Fisher Scientific (Fair Lawn, NJ). Horseradish peroxidase was provided by Boehringer Manheim (Germany), isopropyl-β-D-thiogalactopyranoside by FisherBiotech (Fair Lawn, NJ), and ampicillin by Promega (Madison, WI). Q-Sepharose and 2′,5′-ADP-Sepharose were from Amersham Pharmacia Biotech (Sweden), and the hydroxyapatite gel (Bio-Gel HTP Gel) was from Bio-Rad Laboratories (Hercules, CA). High purity argon (99.998%), CO (99.9%), and the oxygen adsorbent, Oxisorb-W, used to further purify the argon were purchased from Puritan-Bennett Medical Gases (Overland Park, KS). All the chemicals were used without further purification.

Instruments. HPLC was performed on a Hewlett-Packard 1090 Liquid Chromatograph. The UV−visible spectra were recorded on a Hewlett-Packard 8452A diode array spectrophotometer or a Cary 1E Varian UV−visible spectrophotometer. The fluorimeter used was a Perkin-Elmer LS50B. Circular dichroism spectra were obtained on a Jasco J-715 instrument. Resonance Raman spectra were obtained on a McPherson 2061/207 spectrograph (0.67 m with variable gratings) equipped with a Princeton instrument liquid-N_2-cooled (LN-1100PB) CCD detector. Kaiser Optical supernotch filters were used to attenuate Rayleigh scattering. Excitation sources consisted of an Innova 302 krypton laser (413 nm) and a Liconix 4240NB He/Cd laser (442 nm). Spectra were collected in a 90°-scattering geometry on samples at room temperature (cooling the samples to 10 °C with chilled nitrogen gas did not result in any significant change). Frequencies were calibrated relative to indene and CCl_4 standards and are accurate to ± 1 cm^{-1}. CCl_4 was also used to check the polarization conditions. Optical absorption spectra of the Raman samples were obtained on a Perkin-Elmer Lambda 9 spectrophotometer to monitor the sample (fully oxidized, fully reduced, CO complex) both before and after laser illumination.

Engineering of the P450$_{cam}$ C357H Mutant. The pCWori vector provides very good expression of P450$_{cam}$, but works poorly during sequencing and mutagenesis using Quickchange. For this reason, P450$_{cam}$ DNA was cleaved out of pCWori, using *Nde*I and *Xba*I restriction enzymes, and ligated into pUC119 using T4 ligase. Quickchange was then used to prepare the C357H mutant of P450$_{cam}$, with the 5′-sense oligonucleotide 5′-GGC CAC GGC AGC CAT CTG CAC CTT GGC CAG CAC CTG GCC coding for GHGSHLHLGQHLA. Finally, the C357H DNA was cleaved out of pUC119 and ligated into either the standard pCWori vector or to a pCWori vector containing a C-terminal His$_6$-tag. Mutations were confirmed by DNA sequencing.

Fermentations. *Escherichia coli* strain DH5α [*F′ ara* D*(lac-proAB)-rpsLf*80d *lac*ZDM15 *hsd*R17] is transformed with the appropriate plasmid and spread onto Luria-Bernati medium containing agar. One-liter of 2YT liquid medium supplemented with 100 mg/L of ampicillin is used for the mutant. P450$_{cam}$ expression is induced with 1 mM isopropyl-β-D-thiogalactopyranoside at OD$_{600} \sim 0.8$ (that is after about 4 h at 37 °C and 250 rpm), then further grown at 30 °C for 18 h. Unless otherwise specified, all the steps in the protein purification were performed at 4 °C and the enzyme and cells were stored at −78 °C.

Purification of the P450$_{cam}$ C357H Mutant. P450$_{cam}$, putidaredoxin reductase, and putidaredoxin were expressed heterologously in *E. coli* and were purified as reported previously.[59] The purification procedure reported for P450$_{cam}$ affords more than 10 mg of pure and active P450$_{cam}$ per liter of culture, but it is not as successful with C357H. The latter protein is not retained very well by the Q-Sepharose column and undergoes extended proteolysis. The C357H enzyme purity is improved by the use of DEAE instead of Q-Sepharose, even though proteolysis is still observed. The harvested cells (75 g) were lysed for 1 h at 4 °C in 200 mL of 50 mM Tris buffer (pH 7.4) containing 5 mM β-mercaptoethanol, 1 mM EDTA, 200 μM PMSF, 50 mM potassium chloride, 200 μM camphor, and 0.75 g of lysosyme. The cells were further lysed by sonication. Following centrifugation, the 40−60% ammonium sulfate pellets were collected and redissolved in 28 mL of buffer C (50 mM Tris buffer at pH 7.4, 25 mM potassium chloride, and 100 μM camphor), and dialyzed overnight against the same buffer (2 × 4 L). The protein solution was applied to a fast flow DEAE Sepharose column (50 mL) equilibrated with buffer C. The column was first washed with buffer C (100 mL), followed by elution of the protein with buffer D (50 mM Tris buffer at pH 7.4, 300 mM potassium chloride, and 100 μM camphor). The fractions containing the 47 kDa protein were pooled and precipitated with 80% ammonium sulfate. After centrifugation the collected pellets were redissolved in 28 mL of buffer E (40 mM potassium phosphate at pH 7.4 and 100 μM camphor) to get a final ammonium sulfate concentration of about 20%. The sample was loaded onto a phenyl Sepharose column (20 mL) equilibrated with buffer E. The column was washed with 100 mL of buffer E and eluted with a linear gradient increasing from 0 to 20% ammonium sulfate (200 mL). The fractions containing the 47 kDa protein were pooled and dialyzed overnight against buffer E (2 × 4 L). The sample was then concentrated using an Amicon cell with a YM10 membrane and reconstituted as follows. Under argon, 1 mL of hemin solution (24 mg of hemin in 330 μL of 0.1 M NaOH diluted in 30 mL of 100 mM potassium phosphate at pH 7.4) was added to 600 μL of 200 μM C357H (5.7 mg), 75 μL of 0.2 M camphor, and 20 mL of buffer D. The mixture was gently stirred mechanically under argon at room temperature. Small aliquots were taken periodically to monitor the concentration of heme-bound protein (CO-reduced spectrum, $\epsilon_{420} \sim 100$ mM^{-1} cm^{-1}). The optimum heme-bound protein concentration (about 30% based on A_{420} of the CO-reduced spectrum and on A_{280} of the ferric enzyme) was achieved after approximately 18 h when the protein was not tagged. The excess hemin was removed by use of a hydroxyapatite column (40 mL) equilibrated with buffer G (10 mM potassium phosphate at pH 7.4 and 100 μM camphor). The column was washed with 40 mL of buffer G, which elutes a first red band. A second red band was eluted with a gradient increasing linearly from 10 to 200 mM potassium phosphate (400 mL). Both 47 kDa red bands were pooled and concentrated separately using an Amicon cell with a YM10 membrane. From the combined yields of bands 1 and 2, 1 mg of ∼30% heme-bound protein was obtained from reconstitution of 20% of the sample.

Purification of the P450$_{cam}$ C357H-His Mutant and P450cam-His. Because extended proteolysis occurs during the purification of C357H, it was desirable to make the isolation process faster and more efficient. The addition of six histidines at the N-terminus of the protein allowed a faster purification and minimized the amount of proteolysis. The harvested cells (80 g) were lysed for 1 h at 4 °C in 180 mL of 50 mM Tris buffer (pH 7.4) containing 5 mM β-mercaptoethanol, 1 mM EDTA, 200 μM PMSF, 50 mM potassium chloride, 200 μM camphor, and 0.8 g of lysosyme. The cells were further lysed by sonication. Following centrifugation, the supernatant was directly loaded onto a nickel column (20 mL) equilibrated with buffer H (20 mM Tris buffer at pH 8.0, 0.5 M NaCl, 10% glycerol, and 1 mM PMSF). The column was washed with buffer H (120 mL) and the protein was eluted with a linear gradient increasing from 0 to 40 mM imidazole (60 mL). The colored fractions were pooled and dialyzed overnight against buffer E (4 L). Following concentration to 7.5 mL using an Amicon cell with a YM10 membrane, 10% of the protein (800 μL, 185 mg) was reconstituted as described above for C357H. This time, after 18 h of reaction at room temperature, and after removal of excess hemin, 180 mg of heme-bound protein was obtained. On the basis of A_{420} of the CO-reduced spectrum and A_{280} of the ferric enzyme, it was calculated that the reconstitution of C357H-His yielded 50 to 100% heme-bound protein. The heme:protein ratio was found to slowly decrease over time with both the wild-type and the mutant. These results were confirmed using the standard hemochromogen assay for hemin combined with the Bio-Rad protein assay.

UV Characterization of the P450$_{cam}$ C357H and C357H-His Mutants, Electron Transfer, and Determination of the K_d Values. The protein concentration was determined using either $\epsilon_{280} \sim 94$ mM^{-1} cm^{-1} for the ferric state or the Bio-Rad DC Protein assay, based on a comparison with standard curves using albumin as the protein. The heme-bound protein concentration was calculated from the $Na_2S_2O_4$ CO-reduced difference spectrum using $\epsilon_{420} \sim 100$ mM^{-1} cm^{-1}. The transfer of electrons from Pd/PdR/NADH to C357H, C357H-His, P450$_{cam}$, or P450$_{cam}$-His was verified by UV as follows. A mixture of enzyme (1 μM), Pd (4 μM), PdR (1 μM), and camphor (4 μM), through

(59) De Voss, J. J.; Sibbesen, O.; Zhang, Z.; Ortiz de Montellano, P. R. *J. Am. Chem. Soc.* **1997**, *119*, 5489−5498.

which CO had been bubbled, was used as the baseline. When NADH (300 mM) was added, the resulting spectra showed a medium band at 450 nm for P450$_{cam}$ and a weak band at 420 nm for C357H (Figure 6). K_d values for the association of Pd or camphor with P450$_{cam}$-His or the C357H-His mutant were determined using UV spectroscopy by monitoring the decrease in absorbance at 392 nm for the wild-type and 425 nm for the mutant. Pd (0 to 100 μM) or camphor (0 to 50 μM) were added to a solution of the enzyme (2 μM) and camphor (if needed −1 mM) in 10 mM potassium phosphate, pH 7.4, and room temperature.

Determination of the Effect of Different Parameters on the Spin State of the C357H-His Mutant. Unless otherwise indicated, the concentrations used were the following: 1 μM of enzyme, 50 mM of potassium phosphate buffer at pH 7.4 (same concentration and pH when other buffers are tested), and 1 mM of camphor with C357H or 100 μM with P450$_{cam}$. The different buffers compared were potassium phosphate, Tris, Mops, HEPES, ammonium acetate, and sodium citrate. The temperature was varied from 4 to 56 °C, and the pH from 3 to 9. The concentration ranges used were the following: 1 to 10 μM of enzyme, 0 to 100 mM of potassium phosphate buffer, and 0 to 2 mM of either camphor or imidazole. The P450$_{cam}$ high spin state absorbs at 392 nm and the low spin at 416 nm. On the other hand, the high spin state of the C357H mutant absorbs at 418 nm and the low spin at 368 nm.

Determination of the Reduction Potentials of P450$_{cam}$-His Wild-Type and Its C357H-His Mutant. The reduction potentials were determined according to the method described by Massey.[60] The proteins, either wild-type or C357H, were reduced in the presence of Pd from Fe^{III} to Fe^{II} with the oxidation of xanthine to urate using xanthine oxidase as the source of electrons. Benzyl viologen was present as an electron-transfer mediator and indigo carmine ($E° = -158$ mV) was used as a reduction potential indicator. The following mixture (400 μL) was combined in an anaerobic cuvette: enzyme (10 μM), xanthine (250 μM), indigo carmine (10 μM), benzyl viologen (2 μM), camphor (500 μM with wild-type and 2.5 mM with C357H), Pd (5 μM), and EDTA (10 mM) in CHELEX treated 50 mM potassium phosphate buffer at pH 7.4. Xanthine oxidase (200 μL of 10 nM) was placed in the sidearm and the cuvette was made anaerobic by repeated cycles of evacuation and flushing for at least 60 min with high-quality argon purified through an oxygen adsorbant. The spectrum of the solution was recorded and reduction was initiated by adding the xanthine oxidase from the sidearm into the other components in the cuvette (to give a total volume of 600 μL). The Nernst equation was applied to calculate the reduction potential, and the concentration of reduced enzyme was determined at one of the putidaredoxin isosbestic points ($\epsilon_{480} = 25.5$ mM^{-1} cm^{-1}).

NADH Consumption Assay for P450 Enzymes. To a mixture of enzyme (1 μM), Pd (4 μM), PdR (1 μM), and camphor (3 mM) in 50 mM of Tris or potassium phosphate buffer at pH 7.4 was added NADH (200 μM). The consumption of NADH ($\epsilon_{340} \sim 6.2$ mM^{-1} cm^{-1}) was monitored at 340 nm every 0.1 min for 1 min and the activity was calculated from the initial slope.

Transformation of Camphor by P450$_{cam}$, P450$_{cam}$-His, C357H, and C357H-His in the Presence of Pd/PdR. A 500 μL mixture of enzyme (1 μM), Pd (4 μM), PdR (1 μM), camphor (1 mM), and NADH (150 μM) in 50 mM potassium phosphate buffer, pH 7.4, was left at room temperature for 30 min. Two control reactions were run: one without enzyme and one without NADH. When the enzyme was the C357H mutant, more enzyme was used (about 200 μM was required to see any reaction), and catalase (100 μg/mL) was added to consume H_2O_2 resulting from uncoupling. The reaction was tested after 2, 4, 6, and 16 h at room temperature, or at 10 °C overnight. The reaction mixture was extracted with CH_2Cl_2 (2 × 200 μL) and the combined organic layers were evaporated to less than 10 μL before injection on a DB-17, 0.25 μm, 30 m × 250 mm GC column. The temperature was 250 °C at the injector, 300 °C at the detector, and initially 80 °C in the oven. The oven temperature was kept at 80 °C for 1 min, raised to 200 °C at a rate of 10 °C per min, then to 300 °C at a rate of 20 °C per min, and kept at that temperature for 3 min. Under these conditions, camphor elutes in 8.4 min, 5-ketocamphor in 11.3 min, and 5-*exo*-hydroxycamphor in 12.9 min. The GC was, in some experiments, coupled to a low-resolution electron impact mass spectrometer.

Transformation of Camphor by P450$_{cam}$, P450$_{cam}$-His, C357H, and C357H-His in the Presence of H_2O_2. A 500 μL mixture of enzyme (1−300 μM, with the mutant the product was observed at 200 μM or more), camphor (1 mM), and H_2O_2 (700 mM) in 50 mM potassium phosphate buffer at pH 7.4 was left at room temperature or at 10 °C for 2 to 16 h. A control was performed without the enzyme. The mixture was treated in the same way as described above for the transformation of camphor in the presence of Pd/PdR.

Uncoupling Rate of the C357H-His Mutant. The uncoupling rate is followed by monitoring the decrease in fluorescence of scopoletin as H_2O_2 is produced in the presence of horseradish peroxidase.[61] The required scopoletin solution (50 μM) was prepared from a 250 μM stock solution of 9.6 mg of scopoletin in 2% methanol, 150 mM KCl, 10 mM $MgCl_2$, and 50 mM potassium phosphate at pH 7.4. A calibration curve was prepared with triplicate standard solutions containing 0, 5, 10, 15, 20, and 30 μM of H_2O_2. A solution (total volume 300 μL) containing the enzyme (1 μM), camphor (23 μM), Pd (1 μM), and PdR (1 μM) in CHELEX treated 50 mM potassium phosphate buffer at pH 7.4 was preincubated at room temperature. The reaction was started by the addition of NADH (150 μM) and quenched at time intervals ranging from 0 to 200 s by reacting for 2 min at room temperature with scopoletin (300 μL) and horseradish peroxidase (30 μL of a 400 μg/mL solution in buffer). Mixtures were diluted to 10 mL with sodium borate buffer (75 mM at pH 10). The solution (300 μL) was further diluted with more of the same buffer (300 μL) into the cuvette. The fluorescence was quickly measured at 460 nm after excitation at 350 nm. The uncoupling rate thus measured corresponds to the rate of H_2O_2 production.

Peroxidase Aactivity of the C357H-His Mutant. A solution of enzyme (10 μM) and guaiacol (2 mM) in 100 mM potassium phosphate at pH 7.4 was preincubated at 37 °C before the reaction was initiated by the addition of H_2O_2 (2 mM). The peroxidase activity was monitored at 470 nm ($\epsilon_{470} = 3.8$ mM^{-1} cm^{-1}), and the initial rate of guaiacol oligomer formation was used to calculate the activity.

Acknowledgment. We thank Dr. Sun Yuequan for his assistance with the GC-MS experiments. This research was supported by National Institutes of Health grants GM25515 (P.R.O.M.) and GM18865 (Thomas M. Loehr). The mass spectrometric data were obtained in the University of California Biomedical Mass Spectrometry Facility (A. Burlingame, Director) supported by National Institutes of Health Grants NCRR BRTP PR01614 and 5 P30 DK26743.

JA0040262

(60) Massey, V. A simple method for the determination of redox potentials. In *Flavins and Flavoproteins*; Curti, B., Ronchi, S., Zanetti, G., Eds.; Walter de Gruyte & Co.: Berlin, Germany, 1991.

(61) Hildebrandt, A. G.; Roots, I.; Tjoe, M.; Gerhard, H. *Methods in Enzymology*; Fleischer, S., Packer, L., Eds.; Academic Press Inc.: New York, 1974; Vol. 52, pp 342−350.